BRIEF REPORT

Stability of SARS-CoV-2 and other airborne viruses under different stress conditions

Marcilio Jorge Fumagalli[1] · Carlos Fabiano Capato[1] · Luiza Antunes de Castro-Jorge[1] · William Marciel de Souza[1] · Eurico Arruda[1] · Luiz Tadeu Moraes Figueiredo[1]

Abstract

Viral stability under stress conditions may directly affect viral dissemination, seasonality, and pathogenesis. We exposed airborne viruses, including severe acute respiratory syndrome coronavirus 2 (SARS-CoV-2), mumps virus, coxsackievirus B5, human rhinovirus A16, and respiratory syncytial virus, to different temperatures, UV light exposure time, pH values, and osmotic pressures and measured the remaining viral infectivity. Reduced thermal stability was observed for coxsackievirus B5 at 45 °C, while SARS-CoV-2 demonstrated residual infectivity at 55 °C. UV light exposure was an efficient means of viral inactivation but was less efficient for non-enveloped viruses. Rhinovirus A16 and respiratory syncytial virus demonstrated extreme sensitivity to acid conditions, while SARS-CoV-2, rhinovirus A16, and respiratory syncytial virus were unstable in an alkaline environment. The information obtained in this study will be useful for the development of viral inactivation methods and may be correlated with epidemiological and seasonal viral characteristics.

Introduction

The rapid and continuous spread of airborne viruses represents a great challenge to the global health system. Many different strategies have been proposed to prevent airborne disease transmission [1]. Airborne viruses are primarily disseminated by infected individuals via droplets and aerosols that can remain infectious in the environment over time until reaching a susceptible individual [2]. Aerosol-transmitted viruses include many human pathogens of significant clinical importance, including a broad range of viruses from different viral families with diverse genomic compositions, viral particle structures, seasonality of circulation, and modes of transmission. They are responsible for infecting cells of the respiratory tract, mainly causing respiratory-related symptoms, and they have a significant impact on human health and the worldwide economy [3, 4].

Environmental factors such as temperature, ultraviolet radiation, pH, and osmotic pressure may directly affect viral stability and viability and therefore play an important role in viral transmissibility. These factors may induce conformational changes in viral structural proteins, disrupt the viral lipid envelope, or degrade nucleic acids, leading to inactivation of the virus [5, 6]. Understanding the stability and persistence of viral pathogens may have an important impact on elucidating modes of virus transmission, especially in public spaces or in healthcare facilities, where transmission is disproportionally likely to occur [7]. Moreover, it may contribute to the development of inactivation protocols for research, which, while providing safety, should not be overly destructive to virion components, preserving essential properties such as particle and protein structure, protein activity, and genetic integrity.

It is important to assess the relative contribution of different physical and chemical determinants of stability of airborne viruses in order to understand the dynamics of viral transmission in a population, and knowing the properties of virions may help in the development of inactivation methods. In this study, we measured changes in the infectivity of important airborne viruses under different stress conditions, including different temperatures, pH values, UV light exposure, and osmotic pressure.

Handling Editor: Sheela Ramamoorthy.

✉ Marcilio Jorge Fumagalli
marcilio_jorge@hotmail.com; marcilio@usp.br

1 Virology Research Center, Ribeirão Preto Medical School, University of São Paulo, Av. Bandeirantes 3900, Vila Monte Alegre, Ribeirão Preto 140490-900, Brazil

Materials and methods

Viruses and titration assay

The viral strains used in this study were severe acute respiratory syndrome coronavirus 2 (SARS-CoV-2) lineages B (GenBank accession no. MT350282) and P.1 (GISAID accession no. EPI_ISL_2499748), respiratory syncytial virus Long strain (ATCC VR-26), coxsackievirus B5, human rhinovirus A16, and mumps virus (ATCC VR-106). Viral stocks were produced *in vitro* using permissive and susceptible cell lines. Briefly, Vero E6 (SARS-CoV-2 and mumps virus), HeLa-I (coxsackie B5 and human rhinovirus 16) or HEp-2 (respiratory syncytial virus) cells were cultivated in a T-75 flask at 37 °C in a 5% CO_2 atmosphere using Dulbecco's modified Eagle medium (DMEM) supplemented with 10% fetal bovine serum (FBS) until 90-100% confluence. Then, the cell culture medium was removed, the cells were washed twice with phosphate-buffered saline (PBS), and the viral inoculum was added to the cell monolayer, followed by incubation for 1 h with gentle rocking at room temperature to allow viral adsorption. As a negative control, cells were inoculated with medium only. Next, 15 ml of DMEM containing 2% FBS was added, and the cells were incubated until a >50% cytopathic effect was observed. Then, the cell culture supernatant was collected and clarified by low-speed centrifugation at $300 \times g$ for 10 min, and aliquots were prepared and kept at -80 °C until use. For virus viability assays, viruses were quantified in three biological replicates and four technical quadruplicates by endpoint titration using the same cells described above. Briefly, 96-well plates were seeded with 10^4 cells per well 1 day prior to viral titration, using DMEM with 10% FBS. The next day, the supernatant was removed, and serial dilutions of viral inoculum were prepared in DMEM with 2% FBS and inoculated in quadruplicate with a final volume of 50 µL per well. The plates were incubated at 37 °C in a 5% CO_2 atmosphere for 3-5 days, depending on the virus, cytopathic effects were visualized, and titers were determined by 50% endpoint titration [8]. All experimental infections with SARS-CoV-2 virus were carried out under biosafety level 3 conditions.

Virus stability assays

In all experiments and for all viruses, we adjusted the initial virus concentration to 10^6-10^7 $TCID_{50}$/mL by dilution in DMEM with 2% FBS. As a negative control, supernatant from uninfected cells was used. For the temperature stress assay, 250 µl of the initial virus dilution was added to a 1.5-mL tube, the cap was closed, and the sample was incubated at different temperatures (4, 25, 35, 45, and 55 °C) in a water bath for 1 or 2 h. For the UV light experiment, 2 mL of virus suspension was added to an open Petri dish (100 mm × 15 mm) and kept on ice for 0, 30, 60, 90, 120, or 300 seconds at a distance of 30 cm beneath a 90-cm-long 8" tubular 30-watt (UV)-C light with a wavelength of 254 nm with an emission strength of 1 mJ/cm^2, collecting 250 µL at each time point to test viral viability. For the pH stress experiment, the initial viral inoculum was diluted 1:10 in filter-sterilized citrate-phosphate buffer with different pH values (3, 5, 7, 9, and 11) or PBS as a control and incubated at room temperature with gentle rocking for 1 h [9]. Similarly, for the osmotic stability assay, the initial viral inoculum was diluted 1:10 in different filter-sterilized sucrose solutions (0%, 1%, 10%, 20%, 40%, and 80% [w/v]), diluted in distilled water, and incubated at room temperature with gentle agitation for 1 h [9]. The sample was then immediately serially diluted and titrated by $TCID_{50}$ assay. The relative viral reduction was calculated as follows:

$$1 - \frac{Log(TCID50\,control) - Log(TCID50\,test)}{Log(TCID50\,control)}$$

Plaque assay

One day before virus titration, 10^5 Vero E6 cells in DMEM with 10% FBS were seeded in each well of a 48-well culture plate. Viral samples were serially diluted tenfold (10^{-1} to 10^{-5}) in DMEM without FBS. The cell supernatant was removed, and the cells were inoculated in duplicate with 50 µl of viral dilutions and incubated for 1 h at 37 °C with gentle rocking. Then, 500 µl of pre-warmed overlay medium (DMEM + 2% FBS with 3% carboxymethylcellulose [CMC]) was added to each well, and the plates were incubated at 37 °C in a 5% CO_2 atmosphere for 4 days. For visualization of plaques, cells were fixed with 2 ml of 10% formaldehyde for 2 h and stained with 1% naphthol blue black for 30 min.

Statistical analysis

Data were plotted and analyzed using GraphPad Prism 8.0.2 software (GraphPad, USA). For multiple-group comparisons, the mixed-effects model (REML) was used, coupled with Tukey's multiple comparisons test, with a 95% confidence interval. Additionally, nonlinear regression was performed using a one-phase decay or dose-response curve with least-squares fit, where appropriate. Differences were considered statistically significant at $P < 0.05$.

Results and discussion

We evaluated the stability of five different airborne viruses of great medical importance, including SARS-CoV-2 isolates of the lineages B and P.1 (Brazilian variant), mumps virus, coxsackievirus B5, human rhinovirus A16, and human respiratory syncytial virus. These viruses were subjected to four different stress conditions: high temperature, ultraviolet (UV) light, high and low pH exposure, and osmotic pressure. In each case, the remaining viral infectivity was measured in cultured cells by titration based on CPE and compared to standard controls.

We analyzed viral infectivity after exposure to different temperatures, ranging from 25 to 55 °C (Fig. 1). Notably, after treatment at 55 °C, we observed infectious virus for both SARS-CoV-2 lineages near the limit of detection, which was confirmed by plaque assay (~100 PFU/ml), suggesting that some viral particles were stable. Accordingly, a similar thermal resistance at 56 °C was reported previously for SARS-CoV-1 [10]. Moreover, it has been reported that total inactivation of SARS-CoV-2 can occur at 70 °C after only 5 minutes of incubation [11]. Also, conservation of the global shape of the viral spike (S) protein is observed at elevated temperatures, despite conformational changes observed in the S1 subunit and in the secondary structure of the receptor binding domain (RBD) of SARS-CoV-2 [12]. This thermal stability of SARS-CoV-2 may potentially represent an important feature that influences its propensity for dissemination [13]. Moreover, coxsackievirus B5 demonstrated a 2-log reduction in its viability at 45 °C after 1 or 2 h of incubation when compared to the other airborne viruses, including enveloped viruses. Considering that picornaviruses (i.e., rhinovirus A16 and coxsackievirus B5) are non-enveloped viruses,

we expected higher viral particle stability under harsh conditions. Indeed, members of the family *Picornaviridae* usually exhibit stability under harsh conditions, such as high pressure and low temperatures [14, 15]. Also, when subjected to 30 to 300 seconds of exposure to UV light, both rhinovirus A16 and coxsackievirus B5 exhibited considerable resistance, while other airborne viruses showed a faster decrease in viability (Fig. 2). Interestingly, SARS-CoV-2 exhibited high sensitivity to UV light after exposure to 300 mJ/cm^2 for 300s. These results and previously reported data indicate that UV light might be an efficient method for inactivation of SARS-CoV-2, especially under high light potency and long periods of exposure [16, 17].

Viral stability was also evaluated at a wide range of pH values (Fig. 3). Rhinovirus A16 and respiratory syncytial virus showed a drastic decrease in viability under acidic conditions, reaching total inactivation at pH 3. Human rhinovirus has long been known to be a pH-sensitive virus, while it has been demonstrated for respiratory syncytial virus that its tertiary and secondary structures seem more stable with less tendency to aggregate at neutral pH values [18, 19]. Interestingly, SARS-CoV-2 was not inactivated at pH 3, in contrast to SARS-CoV-1, which was completely inactivated at low pH [10]. We also observed a complete inactivation of SARS-CoV-2, rhinovirus A16, and respiratory syncytial virus at pH 11. A plausible explanation for SARS-CoV-2 inactivation at basic pH could be an irreversible conformational change in its S protein, as shown previously for murine coronavirus (MHV-A59), which was shown to form viral clumps and lose infectivity at pH 8. Further studies are necessary to elucidate this feature [20]. Interestingly, incubation at different osmotic pressures did not cause significant changes in the viability of any of the viruses studied.

Here, we demonstrate that clinically relevant airborne viruses show a diverse pattern of stability under different
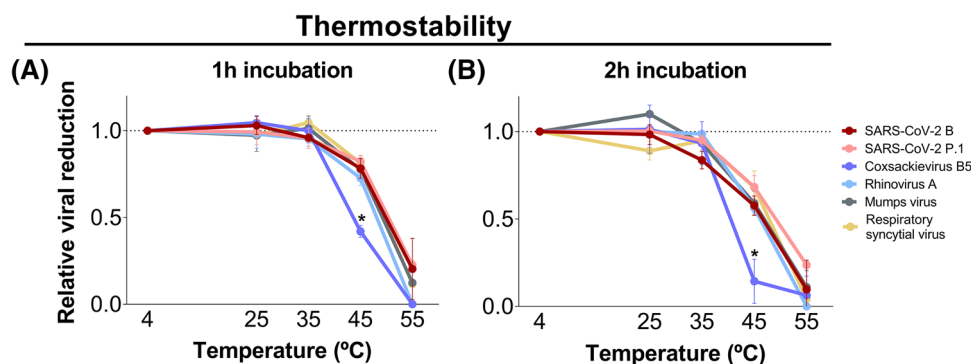

Fig. 1 Thermostability of representative airborne viruses. Virus stability was analyzed at 25 °C, 35 °C, 45 °C, and 55 °C after (A) 1 h or (B) 2 h of incubation. The remaining viral infectivity results were compared to viral titers at 4 °C. '*' indicates a significant difference in viability between coxsackievirus B5 and other viruses (P < 0.05). Viral titers were determined as 50% tissue-culture infectious dose (TCID$_{50}$) per mL, and the data were linearized (LOG$_{10}$) and compared to those obtained with standardized controls. Results are expressed as relative log reduction. Plots show the mean and standard error of three replicates.
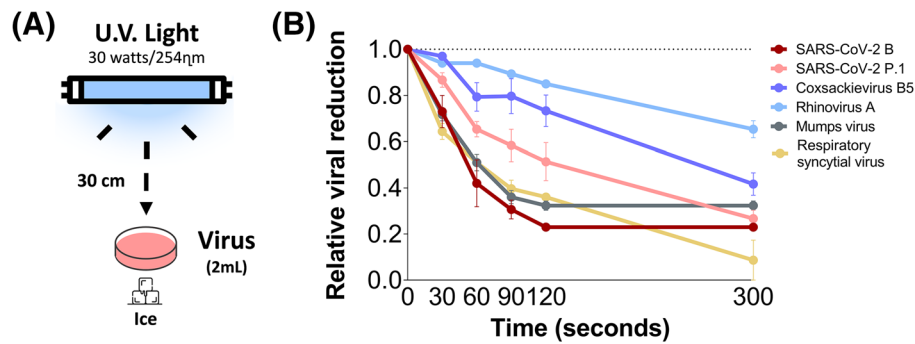
Stability to UV light exposure

Fig. 2 Viral stability under UV light exposure. **(A)** Schematic illustration of the UV light inactivation assay and **(B)** loss of viral infectivity after at 0, 30, 60, 90, 120, and 300 seconds of UV light exposure. Curve-fitting analysis demonstrated that each data set yielded a different curve by one-phase decay with a least-squares fit curve (P < 0.0001). Viral titers were determined as 50% tissue-culture infectious dose ($TCID_{50}$) per mL, and the data were linearized (LOG_{10}) and compared to those obtained for the control. Results are expressed as relative log reduction. Plots show the mean and standard error of three replicates.
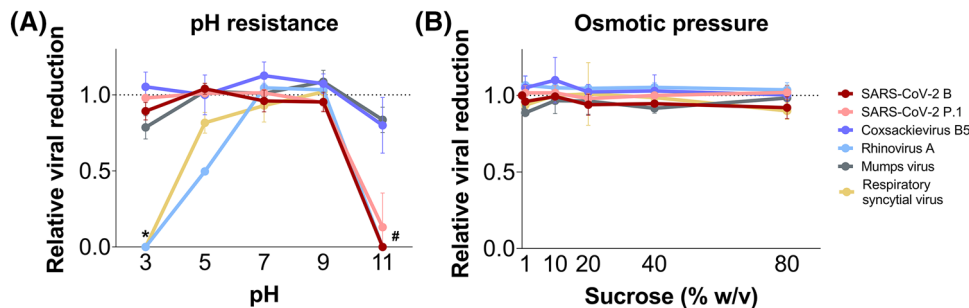
pH and Osmotic pressure

Fig. 3 Viral stability at different pH values **(A)** and osmotic pressures **(B)**. Viral titers were determined as 50% tissue-culture infectious dose ($TCID_{50}$) per mL, and the data were linearized (LOG_{10}) and compared to those obtained for the control. For pH resistance, viruses were incubated for 1 h at a pH of 3, 5, 7, 9, or 11, and the remaining viral infectivity was compared to that of a control treated with PBS. Different detection limits were set for each pH buffer due to cytotoxic effects (pH 3, 6.32×10^2 $TCID_{50}$/mL; pH 5, 7, 9, and 11, 6.32×10 $TCID_{50}$/mL). '*' indicates a significant difference in viability between rhinovirus A16 and respiratory syncytial virus and other groups ($p < 0.05$), '#' indicates significant difference in viability between rhinovirus A16, SARS-CoV-2 lineages B and P.1, and other groups ($p < 0.05$). For osmotic resistance, viral stability was evaluated at different osmotic pressures by incubation in 0%, 1%, 10%, 20%, 40% and 80% (w/v) sucrose. The remaining viral infectivity was compared to that obtained in buffer without sucrose. Results are expressed as relative log reduction. Plots show the mean and standard error of three replicates.

physical and chemical conditions. This report contributes to better understanding of viral transmissibility at a population or individual level, including environmental determinants. Moreover, our data provide supporting information for the development of viral inactivation methods, especially those involving more than one airborne virus. Our results show that common environmental factors may play important roles in viral inactivation and transmission. The parameters evaluated here should be considered when developing viral inactivation protocols or analyzing epidemiological characteristics and viral pathogenesis.

Declarations

Conflict of interest The authors declare no conflict of interest.

References

1. Aliabadi AA, Rogak SN, Bartlett KH, Green SI (2011) Preventing airborne disease transmission: review of methods for ventilation design in health care facilities. Adv Prevent Med 2011:124064
2. Leung NHL (2021) Transmissibility and transmission of respiratory viruses. Nat Rev Microbiol
3. Collaborators GBDLRI (2018) Estimates of the global, regional, and national morbidity, mortality, and aetiologies of lower respiratory infections in 195 countries, 1990–2016: a systematic analysis for the Global Burden of Disease Study 2016. Lancet Infect Dis 18:1191–1210
4. Fendrick AM, Monto AS, Nightengale B, Sarnes M (2003) The economic burden of non-influenza-related viral respiratory tract infection in the United States. Arch Intern Med 163:487–494
5. Boschetti N, Stucki M, Spath PJ, Kempf C (2005) Virus safety of intravenous immunoglobulin: future challenges. Clin Rev Allergy Immunol 29:333–344
6. Wigginton KR, Kohn T (2012) Virus disinfection mechanisms: the role of virus composition, structure, and function. Curr Opin Virol 2:84–89
7. Chang XuH, Rebaza A, Sharma L, Dela Cruz CS (2020) Protecting health-care workers from subclinical coronavirus infection. Lancet Respir Med 8:e13
8. Reed LJ, Muench H (1938) A simple method of estimating fifty per cent endpoints. Am J Epidemiol 27:493–497
9. Griggs TF, Bochkov YA, Nakagome K, Palmenberg AC, Gern JE (2015) Production, purification, and capsid stability of rhinovirus C types. J Virol Methods 217:18–23
10. Darnell ME, Subbarao K, Feinstone SM, Taylor DR (2004) Inactivation of the coronavirus that induces severe acute respiratory syndrome, SARS-CoV. J Virol Methods 121:85–91
11. Chin AWH, Chu JTS, Perera MRA, Hui KPY, Yen HL, Chan MCW, Peiris M, Poon LLM (2020) Stability of SARS-CoV-2 in different environmental conditions. Lancet Microbe 1:e10
12. Marti D, Torras J, Bertran O, Turon P, Aleman C (2021) Temperature effect on the SARS-CoV-2: a molecular dynamics study of the spike homotrimeric glycoprotein. Comput Struct Biotechnol J 19:1848–1862
13. Faria NR, Mellan TA, Whittaker C, Claro IM, Candido DDS, Mishra S, Crispim MAE, Sales FC, Hawryluk I, McCrone JT, Hulswit RJG, Franco LAM, Ramundo MS, de Jesus JG, Andrade PS, Coletti TM, Ferreira GM, Silva CAM, Manuli ER, Pereira RHM, Peixoto PS, Kraemer MU, Gaburo N, Camilo CDC, Hoeltgebaum H, Souza WM, Rocha EC, de Souza LM, de Pinho MC, Araujo LJT, Malta FSV, de Lima AB, Silva JDP, Zauli DAG, Ferreira ACS, Schnekenberg RP, Laydon DJ, Walker PGT, Schluter HM, Dos Santos ALP, Vidal MS, Del Caro VS, Filho RMF, Dos Santos HM, Aguiar RS, Modena JLP, Nelson B, Hay JA, Monod M, Miscouridou X, Coupland H, Sonabend R, Vollmer M, Gandy A, Suchard MA, Bowden TA, Pond SLK, Wu CH, Ratmann O, Ferguson NM, Dye C, Loman NJ, Lemey P, Rambaut A, Fraiji NA, Carvalho M, Pybus OG, Flaxman S, Bhatt S, Sabino EC (2021) Genomics and epidemiology of a novel SARS-CoV-2 lineage in Manaus, Brazil. medRxiv: the preprint server for health sciences
14. Oliveira AC, Ishimaru D, Goncalves RB, Smith TJ, Mason P, Sa-Carvalho D, Silva JL (1999) Low temperature and pressure stability of picornaviruses: implications for virus uncoating. Biophys J 76:1270–1279
15. Shakeel S, Westerhuis BM, Domanska A, Koning RI, Matadeen R, Koster AJ, Bakker AQ, Beaumont T, Wolthers KC, Butcher SJ (2016) Multiple capsid-stabilizing interactions revealed in a high-resolution structure of an emerging picornavirus causing neonatal sepsis. Nat Commun 7:11387
16. Sabino CP, Sellera FP, Sales-Medina DF, Machado RRG, Durigon EL, Freitas-Junior LH, Ribeiro MS (2020) UV-C (254 nm) lethal doses for SARS-CoV-2. Photodiagn Photodyn Ther 32:101995
17. Storm N, McKay LGA, Downs SN, Johnson RI, Birru D, de Samber M, Willaert W, Cennini G, Griffiths A (2020) Rapid and complete inactivation of SARS-CoV-2 by ultraviolet-C irradiation. Sci Rep 10:22421
18. Ausar SF, Rexroad J, Frolov VG, Look JL, Konar N, Middaugh CR (2005) Analysis of the thermal and pH stability of human respiratory syncytial virus. Mol Pharm 2:491–499
19. Skern T, Torgersen H, Auer H, Kuechler E, Blaas D (1991) Human rhinovirus mutants resistant to low pH. Virology 183:757–763
20. Sturman LS, Ricard CS, Holmes KV (1990) Conformational change of the coronavirus peplomer glycoprotein at pH 8.0 and 37 degrees C correlates with virus aggregation and virus-induced cell fusion. J Virol 64:3042–3050